AMERICAN SOCIETY FOR MICROBIOLOGY | Applied and Environmental Microbiology

Understanding the *Streptococcus mutans* Cid/Lrg System through CidB Function

Sang-Joon Ahn,[a] Kelly C. Rice[b]

Department of Oral Biology, College of Dentistry, University of Florida, Gainesville, Florida, USA[a]; Department of Microbiology and Cell Science, Institute of Food and Agricultural Sciences, University of Florida, Gainesville, Florida, USA[b]

ABSTRACT

The *Streptococcus mutans lrgAB* and *cidAB* operons have been previously described as a potential model system to dissect the complexity of biofilm development and virulence of *S. mutans*. Herein, we have attempted to further characterize the Cid/Lrg system by focusing on CidB, which has been shown to be critical for the ability of *S. mutans* to survive and persist in a nonpreferred oxygen-enriched condition. We have found that the expression level of *cidB* is critical to oxidative stress tolerance of *S. mutans*, most likely by impacting *lrg* expression. Intriguingly, the impaired aerobic growth phenotype of the *cidB* mutant could be restored by the additional loss of either CidA or LrgA. Growth-dependent expression of *cid* and *lrg* was demonstrated to be tightly under the control of both CcpA and the VicKR two-component system (TCS), regulators known to play an essential role in controlling major catabolic pathways and cell envelope homeostasis, respectively. RNA sequencing (RNA-Seq) analysis revealed that mutation of *cidB* resulted in global gene expression changes, comprising major domains of central metabolism and virulence processes, particularly in those involved with oxidative stress resistance. Loss of CidB also significantly changed the expression of genes related to genomic islands (GI) TnSmu1 and TnSmu2, the CRISPR (clustered regularly interspaced short palindromic repeats)-Cas system, and toxin-antitoxin (T/A) modules. Taken together, these data show that CidB impinges on the stress response, as well as the fundamental cellular physiology of *S. mutans*, and further suggest a potential link between Cid/Lrg-mediated cellular processes, *S. mutans* pathogenicity, and possible programmed growth arrest and cell death mechanisms.

IMPORTANCE

The ability of *Streptococcus mutans* to survive a variety of harmful or stressful conditions and to emerge as a numerically significant member of stable oral biofilm communities are essential elements for its persistence and cariogenicity. In this study, the homologous *cidAB* and *lrgAB* operons, previously identified as being highly balanced and coordinated during *S. mutans* aerobic growth, were further characterized through the functional and transcriptomic analysis of CidB. Precise control of CidB levels is shown to impact the expression of *lrg*, oxidative stress tolerance, major metabolic domains, and the molecular modules linked to cell death and lysis. This study advances our understanding of the Cid/Lrg system as a key player in the integration of complex environmental signals (such as oxidative stress) into the regulatory networks that modulate *S. mutans* virulence and cell homeostasis.

Streptococcus mutans, a significant constituent of cariogenic oral biofilms, is capable of withstanding a variety of stressors encountered in the oral cavity. The ability of this bacterium to efficiently and rapidly adjust to the dynamic oral environment is essential for its pathogenic lifestyle. Oxidative stress is one of the most important environmental variables affecting the pathogenic potential of *S. mutans*, as high oxygen concentrations disfavor growth of *S. mutans* and other oral bacteria (1–4). Therefore, in order to fulfill its role as a major component of cariogenic oral biofilms and to sustain its virulence, *S. mutans* must overcome oxidative stress. Oxidation sensing and response constitute a complex yet highly regulated process, particularly because it is cross-regulated with other metabolic pathways, stress responses, and virulence physiology (4, 5). A more complete appreciation of how *S. mutans* survives and persists in a suboptimal aerobic environment is critical to understanding the pathogenicity of cariogenic biofilms and ultimately to uncovering novel therapeutic targets. In this respect, the two paralogously related dicistronic operons, *lrgAB* (SMU_575c-SMU_574c) and *cidAB* (SMU_1701c-SMU_1700c) have been previously identified to be highly regulated and finely tuned when *S. mutans* grows with aeration (6). The *cid* and *lrg* operons encode predicted membrane-associated proteins CidA, CidB, LrgA, and LrgB, and their single or combinatory mutations affect a comprehensive "hit list" of virulence traits, such as autolysis, biofilm development, and the oxidative stress response (6). Specifically, when cultured in an aerobic incubator on agar plates, *S. mutans* Δ*lrgAB*, Δ*cidAB*, and Δ*cidB* mutants were almost completely inhibited in terms of growth (6), while Δ*cidA*, Δ*lrgA*, and Δ*lrgB* mutants showed no inhibition compared with the wild-type strain. Additionally, expression levels of *lrg* and *cid* have been shown to be counterbalanced throughout the growth cycle and in response to the availability of oxygen and glucose, environmental

Received 16 May 2016 **Accepted** 5 August 2016

Accepted manuscript posted online 12 August 2016

Citation Ahn S-J, Rice KC. 2016. Understanding the *Streptococcus mutans* Cid/Lrg system through CidB function. Appl Environ Microbiol 82:6189–6203. doi:10.1128/AEM.01499-16.

Editor: H. Nojiri, The University of Tokyo

Address correspondence to Sang-Joon Ahn, sahn@dental.ufl.edu.

Supplemental material for this article may be found at http://dx.doi.org/10.1128/AEM.01499-16.

TABLE 1 Bacterial strains and plasmids used in this study

Strain or plasmid	Relevant characteristics[a]	Source or reference
Strains		
UA159	Wild type	
Δ*cidA* mutant	Δ*cidA*::npKm	6
Δ*cidB* mutant	Δ*cidB*::npKm	6
Δ*cidAB* mutant	Δ*cidAB*::npKm	This study
Δ*cidA*::ΩKm mutant	Δ*cidA*::ΩKm	6
Δ*lrgA* mutant	Δ*lrgA*::npSp	6
Δ*lrgB* mutant	Δ*lrgB*::npEm	6
Δ*lrgAB* mutant	Δ*lrgAB*::ΩKm	6
Δ*lrgA* Δ*cidB* mutant	Δ*lrgA*::npSp Δ*cidB*::npKm	This study
Δ*lrgB* Δ*cidB* mutant	Δ*lrgB*::npEm Δ*cidB*::npKm	This study
ccpA-deficient mutant	Δ*ccpA*::ΩKm	29
vicK-deficient mutant	Δ*vicK*::npKm	3
UA159 ΩP*ldh-cidAB*	P*ldh-cidAB* integrated into the chromosome of UA159 (strain constitutively expressing *cidAB*)	This study
UA159 ΩP*ldh-lrgAB*	P*ldh-cidAB* integrated into the chromosome of UA159 (strain constitutively expressing *lrgAB*)	This study
184-*cidAB*/UA159	UA159 carrying pIB184::*cidAB* (*cidAB*-overexpressing strain)	This study
184-*cidA*/UA159	UA159 carrying pIB184::*cidB* (*cidA*-overexpressing strain)	This study
184-*lrgAB*/UA159	UA159 carrying pIB184::*lrgAB* (*lrgAB*-overexpressing strain)	This study
184-*lrgA*/UA159	UA159 carrying pIB184::*lrgA* (*lrgA*-overexpressing strain)	This study
Plasmid		
pIB184	Shuttle expression plasmid with constitutive P23 promoter, Em	20

[a] np, nonpolar; p, polar; Km, kanamycin resistant; Em, erythromycin resistant; Sp, spectinomycin resistant.

stimuli that have a profound effect on plaque biofilm development (6). This opposing pattern of *lrg* and *cid* expression was also previously demonstrated in microarray data of *S. mutans* cells exposed to blood plasma, whereby *lrg* expression was upregulated 17-fold and *cid* expression was downregulated 3-fold (7). These observations imply that the *lrg* and *cid* operons may operate as a tightly regulated system, possibly in response to nonpreferred environmental stimuli.

Another important facet of the Cid/Lrg system is the potential ability of these proteins to mediate cell death or lysis in a programmed fashion (8, 9). This is analogous to apoptosis (programmed cell death [PCD]), which occurs during development of multicellular organisms. PCD would be beneficial to the cell population within the biofilm by (i) eliminating distinct subpopulations of cells as part of the "normal" course of biofilm development and/or (ii) as an altruistic response to eliminate bacterial cells damaged by environmental or antibiotic stresses (8). Further support comes from the predicted structural similarities between CidA/LrgA and the bacteriophage-encoded holin family of proteins (6, 10–12). Holins are small membrane proteins that induce formation of holes in the cytoplasmic membrane, which allow for cell leakage and access of phage endolysins to the cell wall, which is rapidly cleaved, leading to cell lysis. Antiholins function to inhibit and finely tune the timing of holin action. Although it has been proposed that the Cid/Lrg system mediates cell death in a holin-like manner (13–15), the molecular details of how Cid and Lrg function to control cell death and lysis, as well as many fundamental questions about the Cid/Lrg system, have not yet been completely elucidated. Our previous studies have shown that the *S. mutans* LrgA/B and CidA/B proteins do have a substantial influence on properties of this organism that would affect its ability to colonize and persist in dental plaque biofilm. In fact, our previous analysis of *cid* and *lrg* mutant phenotypes in *S. mutans* suggests a complex interplay between the gene products of these operons (6, 16). For example, *lrgA* and *lrgB* mutations had opposing effects on *S. mutans* autolysis and sucrose-dependent biofilm, whereas *lrgAB*, *cidB*, and *cidAB* mutants each displayed severe aerobic growth inhibition (6). These data have led us to hypothesize that Cid/Lrg may function as a potentially redundant system in *S. mutans*, which contributes to the integration of complex environmental signals such as oxidative stress into the regulatory networks that modulate virulence and homeostasis. The present study further characterizes the *S. mutans* Cid/Lrg system, particularly by providing additional evidence for a potential functional link between *cid* and *lrg*, as well as for the central role of CidB in the ability of *S. mutans* to respond to excessive oxygen. In order to identify Cid/Lrg-associated mechanisms and pathways, we also analyzed the global impact of CidB on the transcriptomes of *S. mutans* cells, grown anaerobically and aerobically, using RNA sequencing (RNA-Seq). Bioinformatics analysis of functional genes of interest provided further insight into how the Cid/Lrg system may contribute to the cellular physiology and virulence of *S. mutans*. Overall, the data obtained herein address the question of how the Cid/Lrg system is integrated into the strategy of *S. mutans* to survive and persist under nonpreferred oxidative stress conditions.

MATERIALS AND METHODS

Strains, plasmids, and growth conditions. The bacterial strains and plasmids used in the present study are listed in Table 1. All *S. mutans* strains were grown in brain heart infusion (BHI) broth (Difco) as static cultures for overnight cultures or on BHI agar plates at 37°C in a 5% (vol/vol) CO_2 atmosphere. For selection of antibiotic-resistant colonies after genetic transformation, erythromycin (10 μg ml^{-1}), kanamycin (1 mg ml^{-1}), or spectinomycin (1 mg ml^{-1}) was added to the medium, when needed. For aerobic growth assays, overnight cultures were diluted 1:100 in fresh medium and the optical density at 600 nm (OD_{600}) was monitored using a Bioscreen C lab system (Helsinki, Finland) as detailed elsewhere (3). Plain BHI broth (without antibiotics) was used in growth experiments in order

to avoid additional stress. To achieve an anaerobic condition, sterile mineral oil (50 μl per well) was additionally placed on top of the cultures. For RNA-Seq experiments, *S. mutans* cells were cultured in three biological replicates. For aerobic growth, an overnight culture was diluted 1:50 into a 250-ml conical flask containing 50 ml of BHI broth and cultures were grown on a rotary shaker (110 rpm) at 37°C. For anaerobic growth, cultures were incubated without agitation in a BBL GasPak Plus anaerobic system (BD, Franklin Lakes, NJ), as described previously (1).

Construction of *S. mutans* mutant strains. Standard DNA manipulation techniques were used to engineer plasmids and strains (17, 18). *S. mutans* mutants were created using a PCR ligation mutagenesis approach (19) to replace nearly all of the target open reading frame (ORF) with a nonpolar resistance cassette of erythromycin (Em), kanamycin (Km), or spectinomycin (Sp). Transformants were selected on BHI agar containing appropriate antibiotics. Double-crossover recombination into each gene was confirmed by PCR and sequencing to ensure that no mutations were introduced into flanking genes. For construction of strains constitutively expressing either *cid* or *lrg*, we first generated a fragment (ΩKm-P*ldh*) containing a polar kanamycin resistance gene (ΩKm) and an *ldh* promoter region (P*ldh*), replacing the promoter region of either *cid* (P*cid*) or *lrg* (P*lrg*). Briefly, two ~0.5-kb fragments flanking the −35 and −10 sequences of the *cidA* or *lrgA* promoter were amplified by PCR, ligated into the ΩKm-P*ldh* cassette, and used to transform *S. mutans*. For construction of overexpression strains, the genes of interest were amplified from UA159 and cloned into a shuttle expression plasmid, pIB184 (20), in which the gene is driven by a constitutive P_{23} promoter. All *S. mutans* stock cultures were maintained at −80°C in 50% glycerol. For each experiment, UA159 and isogenic mutants were streaked on BHI agar plates, with supplementation of appropriate antibiotics. Agar plates were grown for 48 h at 37°C and 5% CO_2 prior to subculturing of individual colonies in BHI broth.

RNA-Seq. Total RNA was isolated and purified from wild-type strain UA159 and Δ*cidB* cell cultures, grown aerobically and anaerobically in BHI broth, and harvested in mid-exponential phase (OD_{600} = 0.5). To remove 16S and 23S rRNAs from each sample, 10 μg of high-quality total RNA ($A_{260/280}$ > 2.0) was processed twice using the MICROBExpress bacterial mRNA enrichment kit (Ambion, Life Technologies, Grand Island, NY, USA), followed by ethanol precipitation and resuspension in 25 μl of nuclease-free water. cDNA libraries were created from the enriched mRNA samples by using the NEBNext Ultra directional RNA library prep kit for Illumina and NEBNext multiplex oligonucleotides for Illumina (New England BioLabs, Ipswich, MA), according to the instructions from the supplier. The concentration and final quality of cDNA libraries were analyzed on an Agilent TapeStation (Agilent Technologies, Santa Clara, CA, USA). Deep sequencing was performed using the Illumina NextSeq500 platform in single-read format by the NextGen DNA Sequencing Core Laboratory, ICBR, at the University of Florida (Gainesville, FL). Read mapping was performed on a Galaxy server hosted by the research computing center at the University of Florida, using Bowtie for Illumina (version 1.1.2).

Data analyses. Mapped reads per gene were then counted from BAM files using htseq-count, as described previously (21). Count-based differential expression analysis of RNA-Seq data was performed with the R package edgeR on RStudio, as described elsewhere (22). Briefly, a table of read counts of all the open reading frames, excluding all rRNA and tRNA genes, was uploaded into RStudio, and then the statistical procedure of edgeR, which is available as packages of the Bioconductor software development project (23), was employed to call differentially expressed genes. To confirm a subset of the differential analysis results obtained using RNA-Seq, conventional quantitative real-time (qRT)-PCR was employed to measure changes in the mRNA level of each ORF as described above. For first-strand cDNA synthesis, 1 μg of total RNA without rRNA depletion treatment was used in the reverse transcription reaction mix for analysis and validation. For further functional analysis of differentially expressed genes, we first conducted gene annotation enrichment analysis using the DAVID bioinformatics resources 6.7 (http://david.abcc.ncifcrf.gov/), which currently searches for over 40 annotation categories, including gene ontology (GO) terms, protein functional domains, and the KEGG (Kyoto Encyclopedia of Genes and Genomes) pathway (24, 25). To remove and cluster redundant GO terms from the results, we used REVIGO (26), and the results were presented in a table (see Tables 4 and 5 and Table S2 in the supplemental material).

Quantitative real-time PCR (qRT-PCR) analysis. To measure the expression of genes using qRT-PCR, *S. mutans* UA159 and its derivatives were grown in BHI broth at 37°C in a 5% (vol/vol) CO_2 atmosphere. For validation of the RNA-Seq data, cells were harvested in mid-exponential phase (OD_{600} = 0.5). To measure the growth-dependent expression of *cid* and *lrg*, cells were harvested in early (OD_{600} = 0.2) and late (OD_{600} = 0.9) exponential or stationary phase. Extraction of RNA, qRT-PCR, and data analysis were performed as described elsewhere (27). Expression was normalized against an internal standard (16S rRNA).

Statistical analysis. All assays were performed in triplicate with RNA isolated from three independent biological replicates. Student's *t* test was used to compare the data for two groups, and data were considered significantly different if the *P* value was at least ≤0.01.

RESULTS

The *cid* and *lrg* operons appear to be transcriptionally cross-regulated. One of the most interesting findings from our previous studies was that the *cid* and *lrg* operons respond to various environmental stimuli, including oxidative stress, in opposing manners (6, 7), suggesting a potential functional relationship between *cid* and *lrg*. We therefore assumed that understanding the inverse correlation between *cid* and *lrg* expression may be important to characterizing the Cid/Lrg system. To further elucidate the interrelated nature of these two operons, we first measured the level of *lrg* and *cid* expression in various *cid* and *lrg* mutants, respectively, using qRT-PCR, in comparison to that of the wild-type strain. To further clarify the functional interrelatedness of *cid* and *lrg*, we also created an additional *cidAB*-deficient mutant (Δ*cidAB*::npKm) in which both *cidA* and *cidB* were deleted. Given the inverse correlation between *lrg* and *cid* expression throughout the growth cycle (6), expression of *lrg* and *cid* was measured at both early (OD_{600} = 0.2) and late (OD_{600} = 0.9) exponential growth phases of each strain. Interestingly, induction of *lrg* expression at late exponential phase (typically observed in the wild-type strain) was lost in the Δ*cidB* mutant but not in the Δ*cidA* and Δ*cidAB* mutants (Fig. 1A). As observed in previously published studies (6, 16), growth phase repression of *cid* expression occurred in the wild-type strain, but this late-exponential-phase repression was modestly lost in the *lrgA* and *lrgB* mutants (Fig. 1B). However, expression of *cid* in the *lrgAB* mutant resembled that in the wild-type strain (Fig. 1B). Transcriptional perturbation of *cid* and *lrg* in the wild-type strain by constitutively expressing either *cidAB* or *lrgAB* from the *ldh* promoter also resulted in altered expression of the native *lrg* and *cid* operons. As shown in Fig. 2A, when *cidAB* was constitutively expressed from the *ldh* promoter of *S. mutans*, late-exponential-phase induction of *lrg* expression was almost completely repressed, while the effect of the constitutive expression of *lrgAB* on *cid* expression was minimal (Fig. 2B). Taken together, these results suggest that growth-dependent expression of *cid* and *lrg* genes may be transcriptionally linked.

Response of *S. mutans* to oxygen is tightly regulated by CidB. We have previously shown that deficiency of CidAB, or of CidB alone, critically impaired the capability of *S. mutans* to grow under aerobic or oxidative stress conditions, while *cidA* deficiency had no discernible effect on aerobic growth (6), highlighting the dom-

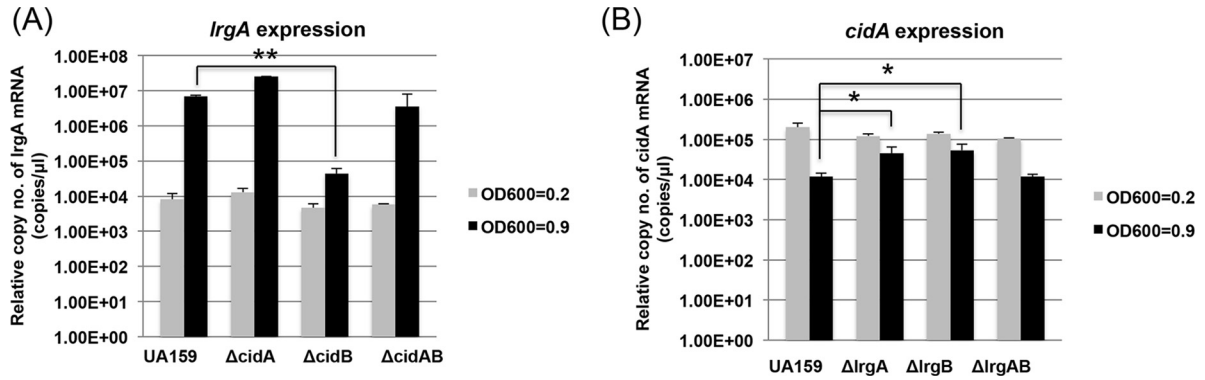

FIG 1 Transcriptional cross-regulation between *lrg* and *cid* operons. The level of *lrg* or *cid* expression was measured using qRT-PCR in *cid* and *lrg* derivative strains, respectively, in comparison to that of the wild-type strain. (A) The expression of *lrgA* was measured at early (OD_{600} = 0.2) and late (OD_{600} = 0.9) exponential growth phases of UA159 (wild type [WT]) and various *cid* mutant strains (Δ*cidA*, Δ*cidB*, and Δ*cidAB*). (B) The expression of *cidA* was measured under the same conditions as those for panel A with UA159 (WT) and various *lrg* mutant strains (Δ*lrgA*, Δ*lrgB*, and Δ*lrgAB*). Data are averages of three independent biological replicates. Differences in relative gene expression between strains were evaluated for statistical significance by Student's *t* test. *, $P < 0.05$; **, $P < 0.005$.

inant role of CidB in the *cid* operon. Interestingly, however, the effect of Δ*cidB* and Δ*cidAB* mutations on *lrg* expression did not follow the same pattern (Fig. 1). Specifically, the *cidAB* deletion mutant had no impact the expression of *lrg*, unlike the *cidB* mutation (Fig. 1A). In fact, the *cidAB*-deficient mutant (Δ*cidAB*::npKm) used above was different from that (Δ*cidA*::ΩKm) used in the previous study (6). Thus, to resolve this issue, we next evaluated the read-through of the terminator in the ΩKm element by measuring the expression of the *cidB* gene downstream of the polar marker (ΩKm) that replaced *cidA* in the Δ*cidA*::ΩKm mutant (6). As shown Fig. 3A, qRT-PCR analysis revealed a 1.2-log reduction in *cidB* expression in the *cidA* polar mutant (Δ*cidA*::ΩKm), whereas a 2.7-log reduction in *cidB* expression was observed in both the Δ*cidB* and Δ*cidAB* mutants, relative to that of the wild-type strain. When *cidA* was replaced by a nonpolar erythromycin marker (Δ*cidA*::npEm), *cidB* expression was identical to that of the wild-type strain. These results suggest that although *cidB* expression was substantially reduced by the ΩKm terminator in the Δ*cidA*::ΩKm strain, the read-through might be sufficient to impact the dissection of phenotypes specific to *cidA* and *cidB*. Measurement of *cidA* expression in each of the *cid* derivative strains confirmed loss of *cidA* in the Δ*cidAB*, Δ*cidA*::ΩKm, and Δ*cidA*::npEm mutants (Fig. 3B). Intriguingly, *cidA* expression was also reduced by about 1 log in the Δ*cidB* mutant (Fig. 3B), suggesting possible autoregulation within the *cid* operon for a balance between *cidA* and *cidB*. More interestingly, either a decrease or a lack of *cidB* expression in the Δ*cidA*::ΩKm and Δ*cidB* mutants, respectively, could upregulate expression of *lrg* (Fig. 3C). Although the changes in *lrg* expression were subtle and not statistically significant in the Δ*cidB* mutant, this result further supports the potential transcriptional linkage between the *cid* and *lrg* operons. Next, to determine whether the differences between the two *cidAB*-deficient strains (Δ*cidA*::ΩKm and Δ*cidAB*::npKm) influence the ability of *S. mutans* in coping with oxidative stress, we reevaluated aerobic growth of these two different *cidAB*-deficient mutants and other *lrg*- or *cid*-deficient strains in BHI liquid medium, as described previously (6). As reported previously, both Δ*cidB* and Δ*cidA*::ΩKm mutants were defective in aerobic growth (Fig. 4A) (6). Interestingly, however, when both *cidA* and *cidB* were completely deleted (Δ*cidAB*), growth of this mutant was identical to that of the wild-type strain (Fig. 4A). Furthermore, mutation of either *lrgA* or *lrgB* alone had no effect on aerobic growth of *S. mutans*, but deficiency in both *lrgA* and *lrgB* critically impaired aerobic growth (Fig. 4B), as described previously (6).

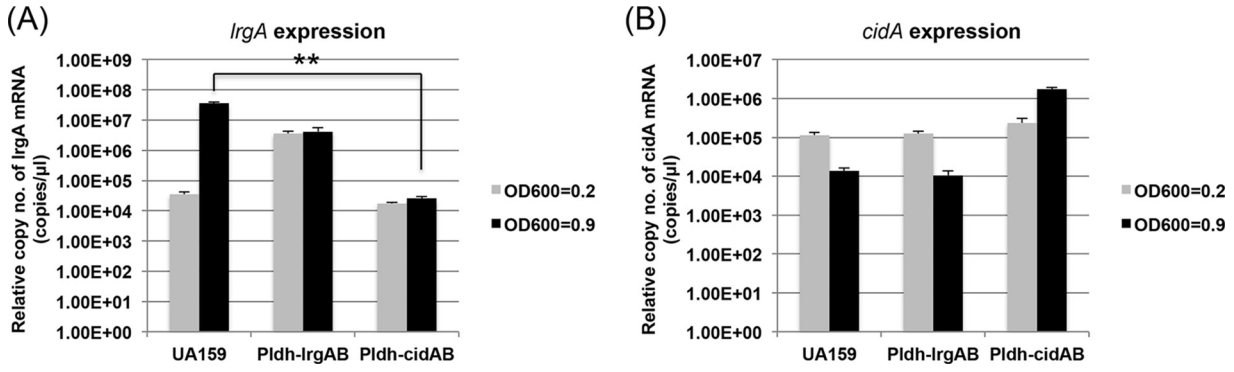

FIG 2 Effect of overexpression of *lrg* or *cid* on *cid* or *lrg*, respectively. The expression of *lrgA* (A) and *cidA* (B) was measured at early (OD_{600} = 0.2) and late (OD_{600} = 0.9) exponential growth phases of UA159 (WT), UA159 ΩP*ldh-lrg*, and UA159 ΩP*ldh-cid* strains by qRT-PCR. Expression of *cid* and *lrg* genes was constitutively driven by the constitutive *ldh* promoter of *S. mutans* in UA159 ΩP*ldh-lrg* and UA159 ΩP*ldh-cid* strains, respectively. Data are averages of three independent biological replicates. Differences in relative gene expression between strains were evaluated for statistical significance by Student's *t* test. **, $P < 0.005$.

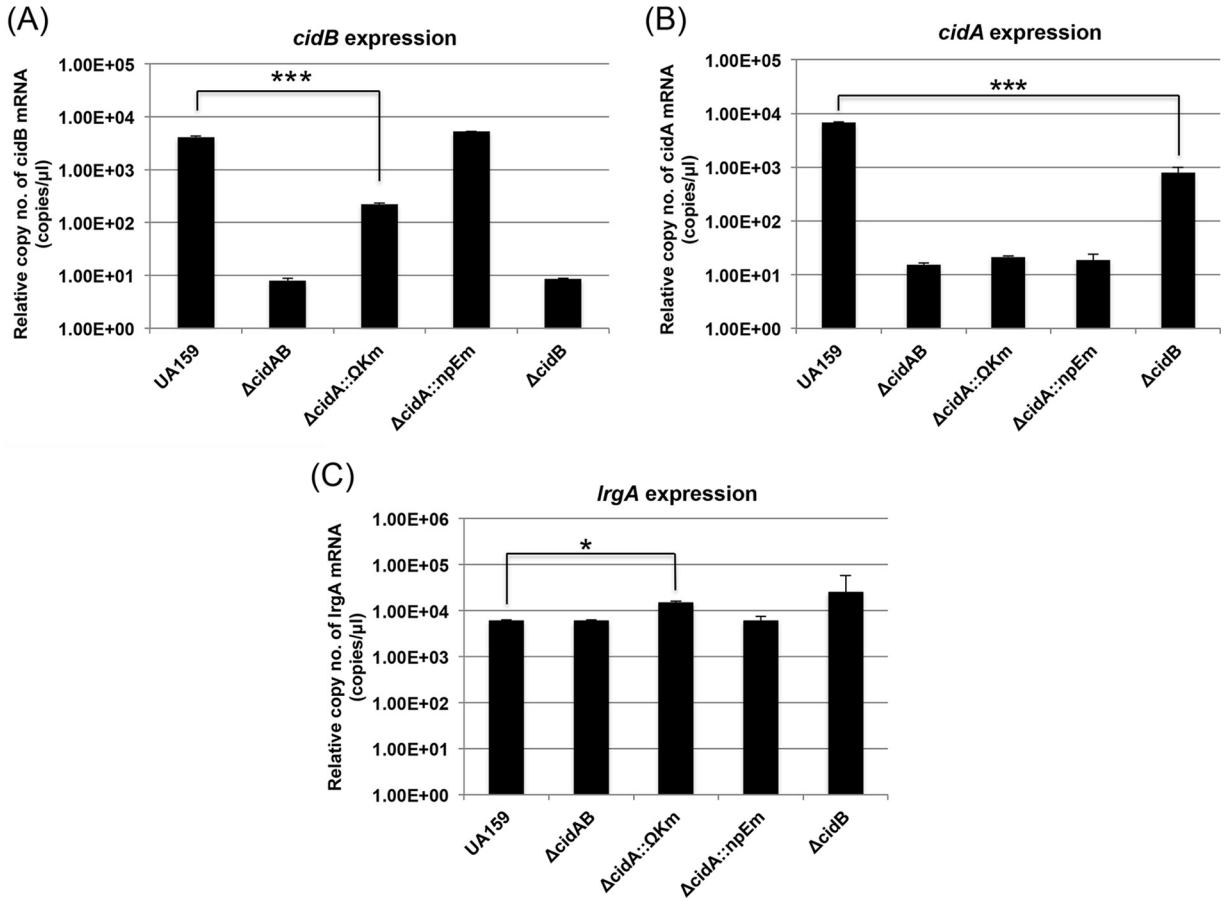

FIG 3 Gene expression determined by qRT-PCR in the *cid* derivative strains. Strains were grown in BHI broth at 37°C in a 5% (vol/vol) CO_2 atmosphere, and cells were harvested in mid-exponential phase (OD_{600} = 0.5). Expression levels of *cidB* (A), *cidA* (B), and *lrgA* (C) were measured and normalized against an internal standard (16S rRNA). Further experimental details are described in Materials and Methods. Data are averages of three independent biological replicates. Differences in relative gene expression between strains were evaluated for statistical significance by Student's *t* test. *, $P < 0.05$; ***, $P < 0.001$.

These results suggest that additional loss of CidA may reverse the effect of a *cidB* mutation or, alternatively, that CidA may be functionally connected with CidB.

A potential functional linkage of CidB and LrgA. Given the potential functional relationship between the *cid* and *lrg* operons, we next addressed whether the *cidB* mutation could be influenced by mutation of *lrg*. For this, we additionally mutated either *lrgA* (Δ*lrgA* Δ*cidB*) or *lrgB* (Δ*lrgB* Δ*cidB*) in the *cidB* background by replacement with nonpolar Sp or Em resistance cassettes, respectively, and then monitored the ability of these mutants to grow under aerobic conditions. Intriguingly, inhibition of aerobic growth by the *cidB* mutation could be substantially rescued by additional mutation of *lrgA* but not as much as when *cidA* was mutated (Fig. 4A). In contrast, mutation of both *cidB* and *lrgB* inhibited aerobic growth of *S. mutans* even more than the *cidB* mutation alone. Therefore, these results suggest that the function of "B" components (CidB and LrgB) might be functionally checked by the "A" components (CidA and LrgA). Although LrgB was not required for aerobic growth of *S. mutans* (Fig. 4A), it was previously shown to affect its growth in the presence of paraquat, a superoxide anion-generating agent (6).

Another possible scenario is that unbalanced expression between the "A" and "B" components of each operon may be toxic under aerobic growth conditions. This interpretation is in line with the previously published observation that *S. mutans* displayed impaired aerobic growth when deficient in either CidAB or CidB alone (6): CidA activity may be "unchecked" in the absence of CidB and may be responsible for this decreased fitness under oxidative stress. To test this, the *cidA* and *lrgA* genes were each cloned under the control of a constitutive promoter (P_{23}) into the shuttle vector pIB184 in the wild-type genetic background. However, the uncontrolled overexpression of *cidA* or *lrgA* had no discernible effect on the aerobic growth of *S. mutans* (Fig. 4A and B). We also investigated the effect of overexpression of *cidAB* (184-*cidAB*/UA159) and *lrgAB* (184-*lrgAB*/UA159) operons in the aerobic growth of the organism. Interestingly, our results showed that overexpression of the *lrgAB* operon caused severe aerobic growth impairment (Fig. 4B) and a moderate difference was found in the *cidAB*-overexpressed strain (Fig. 4A). Therefore, these results suggest that either lack or overexpression of *lrgAB* could be critical to the ability of *S. mutans* to grow in an aerobic environment. In the *cid* operon, only overexpression of *cidAB* seemed to negatively influence the ability of the organism to grow aerobically.

Impact of CidB on the fundamental cellular physiology of *S. mutans*. Next, to provide further insights into the role and regu-

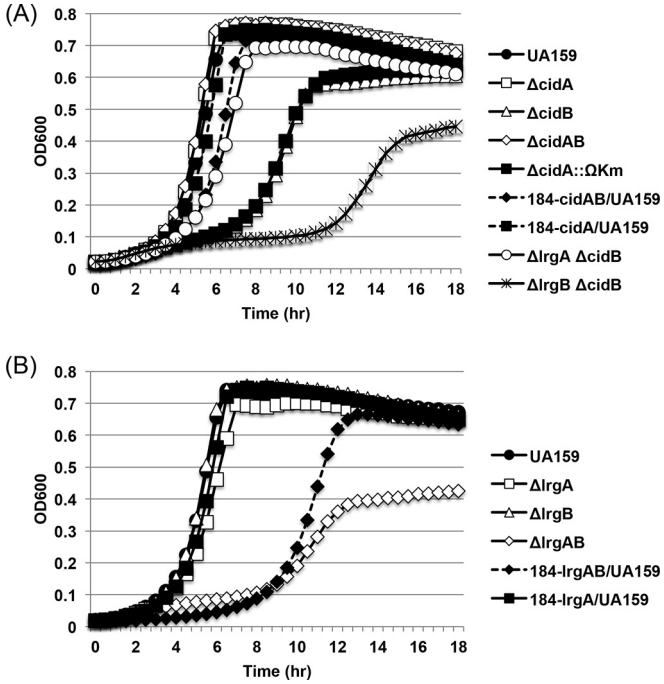

FIG 4 Aerobic growth curves of *S. mutans* UA159 (wild type) and *cid* derivatives (A) or *lrg* derivatives (B). Strains were grown in plain BHI medium. Optical density at 600 nm was monitored every 30 min at 37°C using the Bioscreen C lab system. To achieve relatively aerobic conditions, no sterile mineral oil was placed on top of the cultures. The results are representative of three independent experiments, each performed in triplicate. (A) UA159, wild type; Δ*cidA*, nonpolar *cidA* mutant; Δ*cidB*, nonpolar *cidB* mutant; Δ*cidAB*, nonpolar *cidAB* mutant; Δ*cidA*::ΩKm, polar *cidA* mutant; 184-*cidAB*/UA159, *cidAB* overexpression strain in the wild-type background; 184-*cidA*/UA159, *cidA* overexpression strain in the wild-type background; Δ*lrgA* Δ*cidB*, *lrgA cidB* double nonpolar mutant; and Δ*lrgB* Δ*cidB*, *lrgB cidB* double nonpolar mutant. (B) UA159, wild type; Δ*lrgA*, nonpolar *lrgA* mutant; Δ*lrgB*, nonpolar *lrgB* mutant; Δ*lrgAB*, nonpolar *lrgAB* mutant; 184-*lrgAB*/UA159, *lrgAB* overexpression strain in the wild-type background; and 184-*lrgA*/UA159, *lrgA* overexpression strain in the wild-type background.

lation of the Cid/Lrg system, we employed an RNA-Seq approach to compare the transcriptomes of *S. mutans* wild-type and *cidB* mutant strains under both anaerobic and aerobic growth conditions. To validate the RNA-Seq data, qRT-PCR was performed on a subset of the differentially expressed genes using the same total RNAs of UA159 and *cidB* cells as those used for the RNA-Seq experiment described below. As shown in Table 2, the expression ratio (Δ*cidB* mutant to UA159) for each gene obtained by qRT-PCR was similar to the RNA-Seq results.

UA159 versus Δ*cidB* mutant expression profiles during anaerobic growth. When we compared the transcriptomes of mid-exponential-phase UA159 and Δ*cidB* mutant anaerobic cultures, loss of CidB significantly affected the expression of 105 genes, and more genes were downregulated ($n = 74$) than upregulated ($n = 31$) (cutoff P value of ≤0.005) (Fig. 5A; see Table S1 in the supplemental material). The majority of differentially expressed genes (DEGs) encoded proteins of unknown function or hypothetical proteins (Fig. 5A). Notably, a large number of the DEGs belonged to very few functional groups, including the genomic islands (GIs) TnSmu1 and TnSmu2, the CRISPR (clustered regularly interspaced short palindromic repeats)-Cas system, bacteriocin production, energy metabolism, and amino acid ABC transporters (Table 3). As shown in Table 3, the DEGs were also often structured as operon genes, which would be cotranscribed or coregulated as a single polycistronic mRNA. When the cutoff of ≥1.5-fold change was applied at the same P value, most DEGs belonged to the GIs TnSmu1 and TnSmu2 and CRISPR-Cas, with 11 genes upregulated and 35 genes downregulated (see Table S1). All 25 genes identified within TnSmu1 were 2-fold through 6-fold downregulated in the *cidB* mutant, compared to the wild-type UA159 strain under the anaerobic growth condition (Table 3). In contrast to TnSmu1 genes, all 21 genes identified within TnSmu2 were 1.2-fold or more upregulated, except for SMU_1367c, which was about 2-fold downregulated. Expression of six genes (SMU_1354c to SMU_1356c, SMU_1360c, and SMU_1361c, ≥4-fold upregulated; SMU_1363c, 25-fold upregulated), encoding putative transposes, hypothetical proteins, and a transcriptional regulator, were also highly upregulated in the *cidB* mutant during anaerobic growth (Table 3). These RNA-Seq results also revealed that the CRISPR2-associated *cas* genes, located between SMU_1752 and SMU_1764c, were about 2-fold downregulated in the Δ*cidB* mutant (Table 3; see Table S1), while the CRISPR1-Cas system, located between SMU_1398 and SMU_1405c, was not changed (data not shown). It is also notable that *lrgB* (SMU_574c) was 1.2-fold upregulated in the *cidB* mutant strain (Table 2; see Table S1), confirming the result observed in Fig. 3C and further supporting potential cross-regulation of *cid* and *lrg* expression. Furthermore, expression of SMU_1363c, the most highly upregulated gene in the *cidB* mutant, was measured by qRT-PCR in the other *cid* derivative strains to determine whether its observed differential expression can be corrected to the wild-type level in the Δ*cidAB* strain in the same manner as observed for *lrg* expression in Fig. 1A, 3C, 4A, and 6A. As expected, the SMU_1363c gene was also significantly upregulated in the oxygen-sensitive Δ*cidA*::ΩKm strain to the level observed in the Δ*cidB* strain (see Fig. S1 in the supplemental material). Expression of SMU_1363c was also restored to the wild-type levels in the Δ*cidAB* strain (see Fig. S1). These results suggest that

TABLE 2 qRT-PCR validation of RNA-Seq results

Gene ID	Gene name[a]	Expression fold change (Δ*cidB* mutant/UA159)			
		RNA-Seq		qRT-PCR	
		Anaerobic	Aerobic	Anaerobic	Aerobic
SMU_1363c	*tpn*	24.97	22.2	45.22	18.87
SMU_574c	*lrgB*	1.2	3.78	1.79	1.99
SMU_1396	*gbpC*	1.25		1.51	
SMU_1914c	*cipB*	0.82		0.93	
SMU_423	*nlmD*	0.74		0.82	
SMU_490	*pflC*	0.46		0.55	
SMU_1752	NA	0.4		0.5	
SMU_191	NA	0.19		0.13	
SMU_40	NA		7.08		1.43
SMU_1421	*pdhC*		3.55		1.92
SMU_609	NA		3.33		1.68
SMU_41	NA		3.2		3.02
SMU_82	*dnaK*		2.54		1.39
SMU_925	*cipI*		0.64		0.39
SMU_508	NA		0.45		0.44
SMU_940c	*patB*		0.44		0.38

[a] NA, not available.

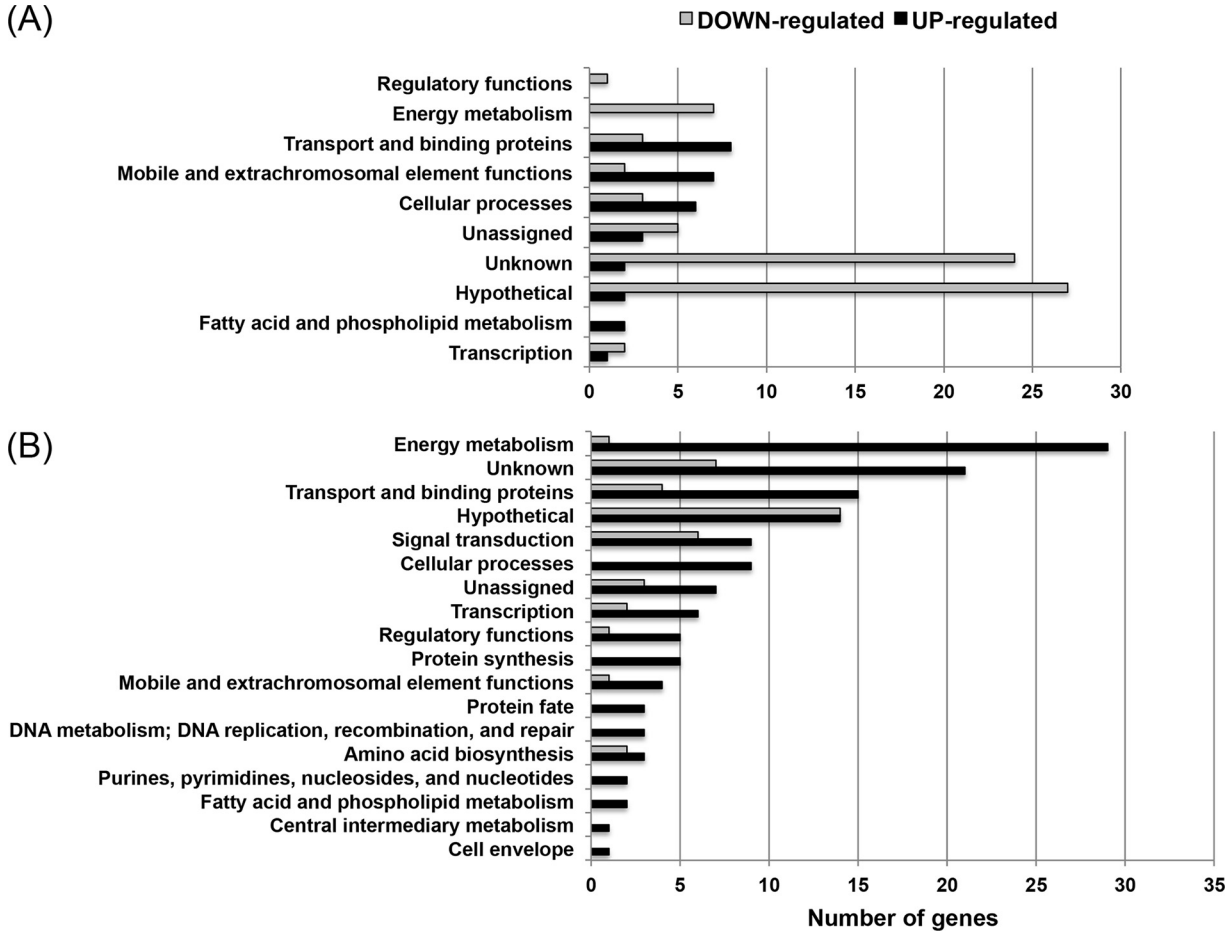

FIG 5 Distribution of functions of genes affected by loss of CidB under anaerobic and aerobic conditions. The 105 (74 upregulated; 31 downregulated) and 180 (41 upregulated; 139 downregulated) genes differentially expressed at a *P* of ≤0.005 under anaerobic (A) or aerobic (B) conditions are grouped by functional classification according to the Los Alamos *S. mutans* genome database (http://www.oralgen.org/).

TnSmu2 genes, including SMU_1363c, may participate in CidB-mediated physiological changes.

In order to gain further insights into the functional activities differentially represented in the absence or presence of CidB during anaerobic growth, we performed enrichment analysis on the DEGs using the DAVID bioinformatics tool (http://david.abcc.ncifcrf.gov/). During anaerobic growth, eight gene ontology (GO) terms, including acyl carrier activity, phosphopantetheine binding, cofactor binding, amine binding, amino acid binding, carboxylic acid binding, vitamin binding, and external encapsulating structure, were significantly (EASE score threshold, <0.05; a modified Fisher exact *P* value) enriched with 31 upregulated genes (see Table S2 in the supplemental material). Significantly changed protein domain terms are also listed in Table S2. In contrast, only one GO term, associated with oxidation reduction, and four protein domain terms were significantly enriched with 74 downregulated genes (see Table S2). No significant genes had a hit on KEGG (Kyoto Encyclopedia of Genes and Genomes) pathway maps. To better understand and remove redundant GO terms from the results, we used REVIGO (26) and enriched GO terms were clustered with representative terms in Table 4.

UA159 versus Δ*cidB* mutant transcriptome changes during aerobic growth. The transcriptomes of the UA159 and Δ*cidB* strains during aerobic growth were also compared, in an attempt to identify the molecular modules or pathways affected by CidB when cells cope with excessive oxygen. With a cutoff *P* value of ≤0.005, loss of CidB affected the expression of 159 total genes. In contrast to the DEGs under the anaerobic growth condition, more genes were upregulated ($n = 140$) than downregulated ($n = 19$) (Fig. 5B) during aerobic growth. As well, a more diverse group of genes was affected in the *cidB* mutant under aerobic growth than under the anaerobic growth condition. Notably, the *cidB* mutation affected a variety of major domains of metabolism, with pronounced changes associated with carbohydrate, amino acid, fatty acid/lipid, nucleotide metabolism, and transport (Fig. 5B; see Table S3 in the supplemental material). Of note, most of the TnSmu1 genes that were downregulated in the *cidB* mutant during anaerobic growth were upregulated under the aerobic condition, with the exception of SMU_191c and SMU_195c (Table 3; see Table S3). In addition, SMU_493 to SMU_495, encoding pyruvate-formate lyase, transaldolase, and glycerol dehydrogenase, respectively, and SMU_2024, encoding a putative transcriptional regulator, were also upregulated in the *cidB* mutant during aerobic growth, in contrast to the anaerobic condition (see Tables S1 and S3). This transcriptional "flipping" of gene expression between the anaerobic and aerobic growth conditions may be related to the

TABLE 3 Interesting gene clusters differentially expressed in UA159 and Δ*cidB* cells when growing under anaerobic conditions[a]

Functional group and gene ID	Expression fold change (Δ*cidB* mutant/UA159)	Gene	Description
TnSmu1			
SMU_191c	0.20	NA	Phage-related integrase
SMU_193c	0.15	NA	Conserved hypothetical protein
SMU_194c	0.21	NA	Conserved hypothetical protein, phage related
SMU_195c	0.13	NA	Hypothetical protein
SMU_196c	0.13	NA	Immunogenic secreted protein (transfer protein)
SMU_197c	0.14	NA	Hypothetical protein
SMU_198c	0.15	*tpn*	Conjugative transposon protein
SMU_199c	0.13	NA	Hypothetical protein
SMU_200c	0.14	NA	Hypothetical protein
SMU_201c	0.14	NA	Conserved hypothetical protein
SMU_202c	0.12	NA	Conserved hypothetical protein; *Streptococcus*-specific protein
SMU_204c	0.12	NA	Hypothetical protein
SMU_205c	0.10	NA	Conserved hypothetical protein
SMU_206c	0.14	NA	Hypothetical protein
SMU_207c	0.15	NA	Transcriptional regulator, Cro/CI family
SMU_208c	0.14	NA	Conserved hypothetical protein, FtsK/SpoIIIE family
SMU_209c	0.13	NA	Hypothetical protein
SMU_210c	0.15	NA	Hypothetical protein
SMU_211c	0.17	NA	Hypothetical protein
SMU_212c	0.19	NA	Hypothetical protein
SMU_213c	0.18	NA	Hypothetical protein
SMU_214c	0.21	NA	Hypothetical protein
SMU_215c	0.19	NA	Hypothetical protein
SMU_216c	0.22	NA	Hypothetical protein
SMU_217c	0.25	NA	Conserved hypothetical protein; *Streptococcus*-specific protein
TnSmu2			
SMU_1339	1.26	*bacC*	Bacitracin synthetase; surfactin synthetase; long-chain fatty acid–CoA ligase
SMU_1340	1.26	*bacA*	Bacitracin synthetase 1/tyrocidin synthetase III
SMU_1341c	1.26	*grs mycB*	Gramicidin S synthase/mycosubtilin synthetase chain MycB; long-chain fatty acid–CoA ligase
SMU_1342	1.25	*bacA*	Bacitracin synthetase; long-chain fatty acid–CoA ligase
SMU_1343c	1.25	*pksC pksL*	Putative polyketide synthase
SMU_1344c	1.21	*fabD*	Malonyl CoA-acyl carrier protein transacylase
SMU_1345c	1.20	*ituA mycA*	Peptide synthetase similar to MycA; long-chain fatty acid–CoA ligase
SMU_1347c	1.91	NA	Permease-ABC-type antimicrobial peptide transport system, permease component
SMU_1348c	1.78	NA	ABC transporter ATP-binding protein
SMU_1351	1.24	NA	Transposase fragment
SMU_1353	1.33	NA	Transposase; mobile element protein
SMU_1354c	4.42	NA	Putative transposase fragment
SMU_1355c	5.18	*tnp*	Transposase
SMU_1356c	4.05	*tpn*	Putative transposase fragment
SMU_1360c	4.64	NA	Hypothetical protein
SMU_1361c	5.02	*yjjB*	Transcriptional regulator, TetR family
SMU_1363c	24.98	*tpn*	Transposase fragment (IS*605*/IS*200*-like); mobile element protein
SMU_1365c	2.01	NA	Permease–FtsX-like permease
SMU_1366c	1.79	NA	ABC transporter ATP-binding protein
SMU_1367c	0.54	NA	Conserved hypothetical protein; methyltransferase
CRISPR/Cas associated			
SMU_1750c	0.58	NA	Hypothetical protein
SMU_1752c	0.40	NA	Hypothetical protein
SMU_1753c	0.41	NA	CRISPR-associated protein Cas2
SMU_1754c	0.45	NA	CRISPR-associated protein Cas1
SMU_1755c	0.45	NA	CRISPR-associated protein Cas1
SMU_1757c	0.48	NA	CRISPR-associated protein Cas1
SMU_1758c	0.47	NA	CRISPR-associated RecB family exonuclease Cas4b
SMU_1760c	0.49	NA	CRISPR-associated protein, Csd2 family
SMU_1761c	0.51	NA	CRISPR-associated protein, Csd1 family
SMU_1762c	0.54	NA	CRISPR-associated protein, Csd1 family
SMU_1763c	0.52	NA	CRISPR-associated protein, CT1134 family
SMU_1764c	0.50	NA	CRISPR-associated helicase Cas3

(Continued on following page)

TABLE 3 (Continued)

Functional group and gene ID	Expression fold change (Δ*cidB* mutant/UA159)	Gene	Description
Bacteriocin associated			
SMU_150	0.77	*nlmA*	Nonlantibiotic mutacin IV A
SMU_151	0.74	*nlmB*	Nonlantibiotic mutacin IV B
SMU_299c	0.74	NA	Bacteriocin peptide precursor
SMU_423	0.75	*nlmD*	Possible bacteriocin
SMU_1914c	0.82	*cipB*	Possible bacteriocin
Amino acid ABC transporters			
SMU_932	1.43	NA	Conserved hypothetical protein
SMU_933	1.41	*atmA*	Amino acid ABC transporter, amino acid substrate-binding protein
SMU_934	1.48	NA	Amino acid ABC transporter, permease protein
SMU_935	1.52	NA	Amino acid ABC transporter, permease protein
SMU_936	1.45	NA	Amino acid ABC transporter, ATP-binding protein
Metabolic pathways			
SMU_137	0.54	*mleS*	Malolactic enzyme
SMU_138	0.58	*mleP*	Malate permease/auxin efflux carrier
SMU_139	0.58	*oxdC*	Oxalate decarboxylase
SMU_140	0.58	*gor gshR*	Glutathione reductase
SMU_141	0.62	NA	Conserved hypothetical protein; integral membrane protein
SMU_490	0.47	*act pflC*	Pyruvate-formate lyase activating enzyme
SMU_491	0.65	NA	Transcriptional regulator, DeoR family
SMU_493	0.52	*pfl pfl-2*	Formate acetyltransferase (pyruvate-formate lyase)
SMU_494	0.55	*mipB talC*	Transaldolase family protein
SMU_495	0.54	*gldA*	Glycerol dehydrogenase

[a] NA, not available; CoA, coenzyme A.

elevated sensitivity of the Δ*cidB* mutant to oxidative stress. In contrast, TnSmu2 genes were upregulated in the *cidB* mutant regardless of the absence or presence of excessive oxygen (Table 3; see Table S3), suggesting an intimate functional linkage between CidB and TnSmu2. Under the aerobic condition, expression of five genes (SMU_101 to SMU_105) in another genomic island, GI-4 (28), was also about 2-fold downregulated in the *cidB* mutant strain (see Table S3). These genes largely encode the components of a phosphotransferase system (PTS). It is also notable that *lrgA* (SMU_575) and *lrgB* (SMU_574) expression levels were more than 3-fold upregulated in the *cidB* mutant, suggesting that CidB may have a greater impact on *lrg* expression during aerobic growth. Importantly, the aerobic RNA-Seq data also suggest that potential Cid/Lrg-mediated cell death mechanisms may be linked with the chromosomal toxin-antitoxin (T/A) modules in *S. mutans*, which are known to inhibit essential bacterial cell functions such as translation or DNA replication. As shown Table S3, two potential toxin-antitoxin (T/A) modules, SMU_173/SMU_172 and SMU_41/SMU_40, were highly upregulated during aerobic growth in the Δ*cidB* mutant in comparison to the wild type. As expected, mutation of *cidB* also led to altered expression of several stress-related loci. For example, SMU_80 to SMU_83, encoding HrcA, GrpE, DnaK, and DnaJ, were significantly upregulated (1.9- to 2.9-fold change). SMU_1954 and SMU_1955, encoding GroEL and GroES, were also upregulated more than 1.5-fold. As shown in Table 5, DAVID and REVIGO analysis of the aerobic growth DEGs revealed that 140 upregulated genes belonged to GO terms related to 23 biological processes (BP), 2 cellular components (CC), 8 molecular

TABLE 4 Gene ontology enrichment analysis of the DEGs from anaerobic RNA-Seq of UA159 versus Δ*cidB* mutant using DAVID and REVIGO tools[a]

Gene category	Term ID and GO	Functional description	EASE score
Upregulated	[GOTERM_CC] GO:0030312	**External encapsulating structure**	2.25E−02
	[GOTERM_MF]		
	GO:0019842	**Vitamin binding**	6.40E−03
	GO:0043176	**Amine binding**	3.87E−04
	GO:0000036	**ACP phosphopantetheine attachment site binding involved in fatty acid biosynthetic process**	6.46E−09
	GO:0048037	**Cofactor binding**	1.20E−04
	GO:0031406	**Carboxylic acid binding**	2.86E−03
	GO:0016597	Amino acid binding	3.87E−04
	GO:0031177	Phosphopantetheine binding	5.77E−06
Downregulated	[GOTERM_BP] GO:0055114	**Oxidation reduction**	3.38E−02

[a] EASE score, a modified Fisher exact *P* value; GO, gene ontology; BP, biological process; CC, cellular component; MF, molecular function; ACP, acyl carrier protein. Bold indicates cluster-representative terms.

TABLE 5 Gene ontology and KEGG pathway enrichment analysis of the DEGs from aerobic RNA-Seq of UA159 versus Δ*cidB* mutant using DAVID and REVIGO tools[a]

Gene category	Term ID and GO	Functional description	EASE score
Upregulated	[GOTERM_BP]		
	GO:0046352	**Disaccharide catabolic process**	2.17E−06
	GO:0005990	Lactose catabolic process	2.31E−05
	GO:0019512	Lactose catabolic process via tagatose-6-phosphate	2.31E−05
	GO:0009313	Oligosaccharide catabolic process	2.17E−06
	GO:0005988	Lactose metabolic process	7.55E−05
	GO:0005984	Disaccharide metabolic process	2.26E−05
	GO:0006084	**Acetyl-CoA metabolic process**	1.01E−02
	GO:0009401	**Phosphoenolpyruvate-dependent sugar phosphotransferase system**	2.20E−05
	GO:0006457	**Protein folding**	1.04E−02
	GO:0045333	**Cellular respiration**	3.90E−02
	GO:0006099	Tricarboxylic acid cycle	3.90E−02
	GO:0009060	Aerobic respiration	3.90E−02
	GO:0030001	Metal ion transport	4.82E−03
	GO:0006812	Cation transport	4.26E−02
	GO:0051187	**Cofactor catabolic process**	3.90E−02
	GO:0009109	**Coenzyme catabolic process**	3.90E−02
	GO:0046356	Acetyl-CoA catabolic process	3.90E−02
	GO:0006811	**Ion transport**	4.24E−02
	GO:0009311	**Oligosaccharide metabolic process**	2.26E−05
	GO:0016052	**Carbohydrate catabolic process**	1.27E−02
	GO:0008643	**Carbohydrate transport**	1.19E−04
	GO:0006814	**Sodium ion transport**	2.06E−02
	GO:0044275	**Cellular carbohydrate catabolic process**	3.62E−03
	[GOTERM_CC]		
	GO:0031224	**Intrinsic component of membrane**	3.13E−02
	GO:0016021	**Integral component of membrane**	4.76E−02
	[GOTERM_MF]		
	GO:0009024	**Tagatose-6-phosphate kinase activity**	2.03E−02
	GO:0015294	**Solute:cation symporter activity**	3.89E−06
	GO:0005351	Sugar:proton symporter activity	7.08E−05
	GO:0005402	Cation:sugar symporter activity	7.08E−05
	GO:0015295	Solute:proton symporter activity	7.08E−05
	GO:0015293	Symporter activity	3.89E−06
	GO:0008982	**Protein-N(PI)-phosphohistidine-sugar phosphotransferase activity**	2.07E−05
	GO:0051119	Sugar transmembrane transporter activity	7.08E−05
	[KEGG_PATHWAY]		
	smu02060	Phosphotransferase system (PTS)	7.78E−06
	smu00020	Citrate cycle (TCA cycle)	1.21E−04
	smu00052	Galactose metabolism	2.94E−04
	smu00620	Pyruvate metabolism	8.86E−04
	smu00051	Fructose and mannose metabolism	1.90E−02
	smu00010	Glycolysis/gluconeogenesis	3.14E−02
Downregulated	[GOTERM_BP]		
	GO:0008643	**Carbohydrate transport**	6.28E−04
	GO:0009401	**Phosphoenolpyruvate-dependent sugar phosphotransferase system**	3.29E−03
	[KEGG_PATHWAY]		
	smu00051	Fructose and mannose metabolism	4.95E−04
	smu02060	Phosphotransferase system (PTS)	7.54E−04
	smu00520	Amino sugar and nucleotide sugar metabolism	9.64E−03

[a] EASE score, a modified Fisher exact *P* value; GO, gene ontology; BP, biological process; CC, cellular component; MF, molecular function; KEGG, Kyoto Encyclopedia of Genes and Genomes. Bold indicates cluster-representative terms.

functions (MF), and 6 KEGG pathways, while two GO (BP) terms and three KEGG pathways were significantly enriched with 19 downregulated genes. Representative GO terms enriched with either upregulated or downregulated genes largely included carbohydrate transport and metabolism (listed in Table 5), suggesting that loss of CidB leads to a global adjustment in major domains of central metabolism when *S. mutans* copes with oxidative stress.

CcpA and VicKR are significantly involved in the expression of *cid* and *lrg*. We have previously demonstrated that growth-dependent changes in *lrgAB* expression are regulated by the LytST two-component signal transduction system (TCS), which is located immediately upstream of *lrgAB* (6). As shown above (Fig. 1A, 2A, and 3C), alteration of cellular CidB levels can also affect expression of *lrg*. Nevertheless, the genetic regulatory circuits gov-

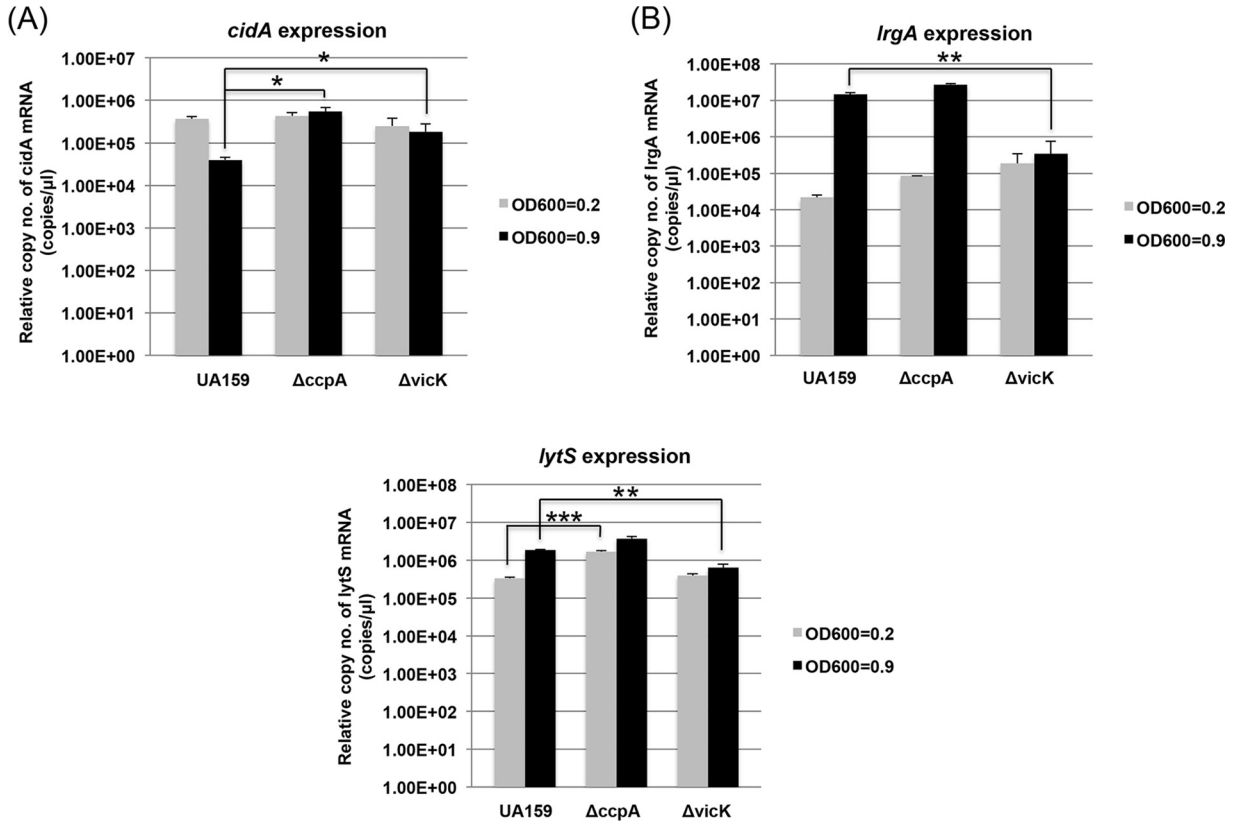

FIG 6 Effect of CcpA and VicK on expression of *S. mutans cid*, *lrg*, and *lytS*. The expression of *cidA* (A), *lrgA* (B), and *lytS* (C) was measured by qRT-PCR at early (OD_{600} = 0.2) and late (OD_{600} = 0.9) exponential growth phases of UA159 (WT), *ccpA*-deficient, and *vicK*-deficient strains. Data represent the averages of three independent biological replicates. Differences in relative gene expression levels between strains were evaluated for statistical significance by Student's *t* test. *, $P < 0.05$; **, $P < 0.005$; ***, $P < 0.001$.

erning *cid* expression still remain poorly characterized. In an attempt to identify the regulatory mechanisms or pathways that control expression of *cid*, we decided to further explore the involvement of CcpA, known to serve as a major regulator of carbon metabolism in *S. mutans* and previously shown to be involved in the expression of *cid* and *lrg* by Northern blot analyses (6). We therefore quantified growth-dependent expression of *cid* and *lrg* in the wild type and *ccpA* (29) mutants using real-time qPCR, under the growth same conditions described above (Fig. 1 and 2). In contrast to the wild-type strain, increased expression of *cidA* at early exponential growth phase (OD_{600} = 0.2) was maintained through the late exponential growth phase (OD_{600} = 0.9) in the *ccpA* mutant (Fig. 6A). However, *lrg* expression was elevated at the late exponential growth phase (OD_{600} = 0.9), similar to that of the parent strain UA159. Nevertheless, the overall expression of *lrg* was moderately increased in the *ccpA* mutant (Fig. 6B), which might be due to elevated expression of *lytST* which has also been observed previously in the *ccpA* mutant (Fig. 6C). These results strongly suggest that expression of *cid* is regulated in a CcpA-dependent manner, which is in strong agreement with the aerobic RNA-Seq data showing a large number of DEGs involved in carbon/energy metabolic pathways (Table 5; see Table S3 in the supplemental material).

Analysis of the aerobic RNA-Seq data also revealed that expression of multiple genes involved in cell wall biosynthesis and metabolism were highly altered in the *cidB* mutant (see Table S3). Thus, we hypothesized that the VicKR TCS, well-known to control cell wall metabolism by effectively coordinating peptidoglycan plasticity with the cell division process in many Gram-positive bacteria (30–36), may be involved in regulation of the *cid* operon, the *lrg* operon, or both. To test if the *cid* and *lrg* genes are under the control of VicKR, we also compared the expression of *lrgA* and *cidA* in a *vicK* mutant (*vicK* deficient) (3) and wild-type strains in the early (OD_{600} = 0.2) and late (OD_{600} = 0.9) exponential phases using qRT-PCR. Interestingly, *cid* expression in the *vicK* mutant did not show the decrease in expression at late exponential phase that was noted in the wild-type strain (Fig. 6A). As well, there was no induction of the *lrg* genes in the *vicK* mutant as the cells entered late exponential phase (Fig. 6B), and *lrg* expression was significantly higher in early exponential phase in the *vicK* mutant than in UA159. The differences in expression patterns of the *lrg* operon in the *vicK* mutant may be explained, at least in part, by the observation that *lytS* operon expression was also altered in the VicK-deficient strain (Fig. 6C). Taken together, these data show that expression and function of *cid* and *lrg* are regulated in a more complex manner than previously thought, involving CcpA and at least two TCS (LytST and VicKR).

DISCUSSION

The present study was geared toward understanding the molecular and cellular bases for the contribution of CidB to the ability of *S. mutans* to cope with oxidative stress, as this may improve our

understanding of how the Cid/Lrg system contributes to this pathogen's persistence and survival in the environmentally dynamic oral cavity. The presented comparisons of wild-type and *cidB* mutant transcriptomes have yielded important clues that will help make potential connections between the *cid* and *lrg* operons, resistance to oxidative stress, and possibly regulation of cell death. Overall, these findings also highlight a potential functional interplay between *cid* and *lrg*, which was previously implicated by the counterbalanced expression of these genes in response to growth phase, glucose, and oxygen levels (6). Notably, loss of either *lrgA* (or *lrgB*) or *cidB* influenced the expression of *cid* or *lrg*, respectively, and constitutive expression of *cid* strongly repressed the stationary-phase induction of *lrg* expression. These results suggest that the Cid/Lrg system may be controlled by a potential cross-regulatory mechanism, resulting in a rapid and balanced modulation of Cid and Lrg activities at the transcriptional level once the organism encounters environmental stresses. If this idea is correct, any resulting unbalance between *lrg* and *cid* may result in a profound impact on *S. mutans* cellular functions, including the ability to grow and survive under stress conditions. A more complex picture emerged when we observed that the *cidB* mutation could be completely or partly restored by additional mutation of either *cidA* or *lrgA*, respectively, and mutation of both "B" components of each operon works additively to increase sensitivity to oxygen, further suggesting that the individual "A" and "B" components of CidAB and LrgAB may also be regulated within the system. Nevertheless, it is still unclear why the Δ*cidAB* and Δ*cidA*::ΩKm strains display opposite phenotypes. In fact, the phenotypes of the Δ*cidA*::ΩKm strains are much closer to those of the Δ*cidB* strains than the Δ*cidAB* strains in that both Δ*cidA*::ΩKm and Δ*cidB* strains have increased sensitivity to oxygen and could induce expression of *lrg*. Interestingly, we also found that the *cidB* mutation positively regulated expression of the *cid* operon, since expression of *cidA* was significantly decreased in the Δ*cidB* strain. Thus, either increased expression of *cidA* or unbalanced expression between *cidA* and *cidB* might be crucial to the phenotypic effects of Cid/Lrg. However, no discernible phenotype, including sensitivity to oxygen, was observed in the *cidA*-overexpressed strain. Although further investigation is needed to mechanistically understand the differences between the Δ*cidAB* and Δ*cidA*::ΩKm strains, the data obtained herein strongly suggest that CidB is tightly regulated in the *S. mutans* Cid/Lrg system. A possible scenario for regulation of *cid* may be that expression of this operon is regulated by positive-feedback autoregulation of the *cid* operon or, alternatively, the Cid/Lrg system and that the level of expression of *cidB* modulates the strength of this potential feedback.

Clearly, the transcriptional linkage between *cid* and *lrg* adds another layer of complexity to the regulation that occurs within the Cid/Lrg system. Given that both Δ*cidA*::ΩKm and Δ*cidB* strains were able to induce *lrg* expression, their phenotypes may be, at least in part, attributed to the elevated level of *lrg* expression. These phenotypes also imply that LrgAB is more active during aerobic growth, which is in line with our previous finding that the *lrg* operon is more highly expressed during aerobic growth (1, 6). Further considering that either lack or overexpression of *lrg* increases sensitivity of *S. mutans* to oxygen, *lrg* expression levels may be an actual determinant of the Lrg/Cid-mediated phenotypes. Therefore, these data support the hypothesis that an optimal balance between the levels of *cid* and *lrg* expression is required for ideal aerobic growth and that these operons are functionally interconnected in as yet unknown ways. Based on these and previously published results, it is likely that both Cid and LytST (6, 16) contribute to regulation of *lrg* expression. In fact, we have previously shown that expression of *lrg* is not completely under the control of LytST, suggesting the presence of an additional regulator(s) that controls *lrg* expression (16). The detailed mechanism for how expression of *lrg* is coordinated by Cid and LytST appears to be an important part of understanding the Cid/Lrg system and warrants further investigation.

From a mechanistic standpoint, it seems significant that *lrg* and, to an even greater extent, *cid* are under the tight control of CcpA, reinforcing the idea that the Cid/Lrg system is coordinated with the metabolic status of *S. mutans*. This concept correlates well with the RNA-Seq data presented in this study of wild-type versus Δ*cidB* aerobic cultures grown in BHI broth (containing 11 mM glucose). This analysis revealed that mutation of *cidB* largely altered the expression of genes associated with major metabolic pathways, including phosphotransferase systems (PTS), the citrate cycle (tricarboxylic acid [TCA] cycle), galactose metabolism, pyruvate metabolism, fructose and mannose metabolism, glycolysis/gluconeogenesis, and amino sugar and nucleotide sugar metabolism. More recently, expression of *cidB* was also shown to be 3-fold upregulated in fructose-grown UA159 cells compared to glucose-grown cells (21). Collectively, these findings suggest that the Cid/Lrg system functions primarily under unfavorable environmental conditions such as glucose limitation and aerobic growth. In the same context, it is also noteworthy that expression of *cid* and *lrg* is under the tight control of the VicKR TCS. VicKR and its homologous TCSs have been reported to be directly and intimately involved in regulating bacterial life and death, primarily by controlling cell wall metabolism (30, 37). Intriguingly, VicKR homologues also share the unusual feature that this TCS is essential for viability in most bacteria possessing this regulatory system (30–36). In line with these studies, a *vicK*-deficient strain was recently shown to enhance cell death and lysis in *S. mutans* (38). Therefore, it is not surprising that the Cid/Lrg pathway, previously postulated to control bacterial cell lysis and death (8, 9), is regulated by VicKR, an attractive target for determining if a controlled cell lysis/death system functions in *S. mutans*. Importantly, VicKR has also been reported to play an important role in oxidative stress tolerance (3, 31, 33, 39), antibiotic resistance (40, 41), and infection and virulence (34–36, 42, 43). In line with this logic, it is highly possible that both the VicKR and holin-like Cid/Lrg systems may contribute to a controlled cell death mechanism, potentially involved in orchestrating the cell wall response to environmental stress. This idea is further supported by a possible role for VicKR in sensing and responding to oxygen levels and/or redox potential, consistent with the presence of a PAS domain (44) in VicK. Combined with our previous and current observations (6, 16), *lrg* expression and *cid* expression appear to be controlled by at least two TCSs (LytST and VicKR) and CcpA. LytST regulates *lrg*, but not *cid*, while VicKR regulates both. In contrast, CcpA is largely involved in *cid* regulation. And as described above, Cid is also able to regulate the function of Lrg. Therefore, our future studies will focus on evaluating the relative contributions of LytT, VicR, and CcpA in governing expression of *lrg* and *cid*, providing a deeper insight for the balanced expression pattern observed between these two operons.

As implicated by the data presented here, it is likely that CidB is a central player in the Cid/Lrg system. Specifically, the RNA-Seq

transcriptomic studies comparing the wild type and the Δ*cidB* mutant have provided further insights into the role and regulation of the Cid/Lrg system. These results have shown that the bulk of genes differentially expressed in the Δ*cidB* strain during anaerobic growth belong to several genomic islands (GIs), such as TnSmu1, TnSmu2, and CRISPR-Cas. Notably, the TnSmu2 genes were previously shown to be downregulated in the strain lacking *lytS*, located upstream of *lrgAB* and known to positively regulate *lrgAB* expression (16). GIs are ubiquitous in prokaryotes and are acquired by horizontal gene transfer (45, 46). They normally carry genes that encode a variety of functions responsible for adapting to a particular set of environmental conditions. TnSmu1 corresponds to a large region of 23 kb spanning from SMU_191c to SMU_226c in strain UA159 and carries the genes that encode predicted integrases, bacteriophage-associated proteins, and transposon proteins (28). Particularly, TnSmu1 genes encode many functionally unknown hypothetical proteins, suggesting that the role and regulation of the GI in *S. mutans* are still far from fully elucidated. TnSMu2 is the largest GI (57 kb) found in the *S. mutans* genome, is reported to contain about 47 genes (28) involved in bacitracin and gramicidin synthesis, and is responsible for nonribosomal peptide and polyketide (NRP/PK) biosynthesis of a pigment that enhances aerobic growth and tolerance to H_2O_2 challenge in UA159 (47). It is also noteworthy that the Cid/Lrg system is connected to the CRISPR (clustered regularly interspaced short palindromic repeats)-Cas (CRISPR-associated) system, known to provide a sequence-based adaptive immunity against mobile genetic elements, such as phages, invasive conjugative plasmids, and transposable elements in bacteria (48–52). The *S. mutans* UA159 genome contains two distinct CRISPR-Cas systems: a type II-A CRISPR1-Cas system and a type I-C CRISPR2-Cas system (53, 54). The *cas* genes were recently reported by Serbanescu et al. to contribute to the ability of *S. mutans* UA159 to persist under various stressful conditions, including cell membrane and oxidative stress, heat shock, and DNA-damaging conditions (53). Given the potential that CidA and LrgA bear a resemblance to phage holins, this observation further suggests that perturbation of the Cid/Lrg system may mimic a phage-induced response. Further efforts are under way to investigate how the CRISPR-Cas is linked with CidB and the Cid/Lrg system in coping with unfavorable environmental conditions. Intriguingly, Serbanescu et al. also reported that the expression of *cas* genes within the CRISPR-Cas systems could be differentially regulated by the VicKR TCS (53), which was also shown to regulate *cid* and *lrg* gene expression in this study. Collectively, these data support a role for the Cid/Lrg system in coping with environmental stressors and mediating cell death and lysis, and the three GIs that were transcriptionally altered in the *cidB* mutant appear to be tightly linked with the Cid/Lrg system.

We were also interested in how the transcriptome of the *cidB* mutant changes under aerobic growth conditions, due to the requirement of CidB for *S. mutans* growth under harsh oxidative conditions. Notably, we found that mutation of *cidB* led to a global readjustment in central metabolism and virulence processes, particularly in coping with oxidative stress. The fact that major carbon metabolic pathways were especially active opens the possibility that CidB or the Cid/Lrg system may serve to prime the cellular response to oxidative stress and/or to ensure survival of a subpopulation in a metabolically adjusted manner. In this regard, it is also possible that CidB may be involved in persister formation, possibly through modulating cellular processes within a population. Persisters constitute a subpopulation of phenotypic variants that are genetically identical and metabolically slow-growing cells in a clonal bacterial population, largely in response to antibiotics (55–57). Recently, other stress responses and particularly oxidative stress were also reported to contribute to persister formation in *Escherichia coli* (58). Thus, this idea is consistent with the potential of the Cid/Lrg system to regulate cell death and lysis in a programmed fashion within a population. The idea is further supported by our RNA-Seq data showing that genes encoding two potential toxin/antitoxin (T/A) modules, SMU_173/SMU_172 and SMU_41/SMU_40, were significantly upregulated in the Δ*cidB* mutant compared to the wild type during aerobic growth. SMU_173/SMU_172 (*mazE/mazF*) has been previously well characterized as a functional type II toxin-antitoxin (T/A) addiction system, consisting of a pair of genes that encode a stable toxin and a labile antitoxin (59). However, the function of SMU_41/SMU_40 is currently unknown. SMU_41 lacks canonical T/A features by sequence homology analysis, although SMU_40 is predicted to encode a putative antitoxin by RASTA-Bacteria (Rapid Automated Scan for Toxins and Antitoxins in Bacteria), a Web-based tool for identifying toxin-antitoxin loci in prokaryotes (60). T/A modules are reported to play a central role in persister formation and/or the persister state (61–63). T/A modules are also known to function as "regulatory switches" under adverse conditions, allowing cells to enter a state that confers protection against a severe stressful condition or nutrient limitation, ultimately contributing to programmed cell death as a bacterial survival strategy (57, 64–66). Given that many genes related to PTS, the major route for internalization of carbohydrates in *S. mutans*, were differentially and highly regulated in the *cidB* mutant strain, it is also possible that the Cid/Lrg system fine-tunes cellular physiology during periods of stress to help preserve normal cellular homeostasis (e.g., during periods of "feast or famine" in oral plaque) through the potential T/A modules. Therefore, in order to improve our understanding of the connections between the Cid/Lrg system and metabolic pathways, a complete metabolomics analysis and comparisons of wild-type and Δ*cidB* cultures constitute an attractive approach and are under way in our research group.

In conclusion, our data suggest that the Cid/Lrg system is regulated in a more complex manner than previously expected, involving at least two TCSs (LytST and VicKR), CcpA, and potential cross talk/regulation between the *cid* and *lrg* operons themselves. However, due to the functional and genetic interplay between *cid* and *lrg* operons, it is difficult to establish direct correlations between the observed phenotypes of some of these mutants. Nevertheless, it seems that both *cid* and *lrg* work together when *S. mutans* is challenged by environmental stresses, although we still do not understand how the *cid* and *lrg* gene products are functionally related. In the present study, we were able to probe changes in the transcriptome of *S. mutans* in great depth and with great sensitivity as a function of exposure to oxygen, by using RNA-Seq. The transcriptomic analysis of wild-type versus *cidB* mutant strains revealed potential effects of CidB on various predicted cellular processes. Given the global effects of CidB on the metabolic pathways and stress response of the organism, future study of the Cid/Lrg system has the potential to disclose how complex environmental signals are integrated into the regulatory networks modulating *S. mutans* virulence and homeostasis at the cellular and/or community level.

ACKNOWLEDGMENTS

We thank members of the Burne laboratory, including Lin Zeng, for technical assistance with RNA-Seq experiments.

This work was supported by NIH-NIDCR grants R03 DE023604 (S.-J.A.) and R01 DE025237 (S.-J.A.).

FUNDING INFORMATION

This work, including the efforts of Sang-Joon Ahn, was funded by HHS | NIH | National Institute of Dental and Craniofacial Research (NIDCR) (R03 DE023603 and R01 DE025237).

REFERENCES

1. **Ahn SJ, Wen ZT, Burne RA.** 2007. Effects of oxygen on virulence traits of *Streptococcus mutans*. J Bacteriol **189:**8519–8527. http://dx.doi.org/10.1128/JB.01180-07.
2. **Ahn SJ, Ahn SJ, Browngardt CM, Burne RA.** 2009. Changes in biochemical and phenotypical properties of *Streptococcus mutans* growing with aeration. Appl Environ Microbiol **75:**2517–2527. http://dx.doi.org/10.1128/AEM.02367-08.
3. **Ahn SJ, Burne RA.** 2007. Effects of oxygen on biofilm formation and the AtlA autolysin of *Streptococcus mutans*. J Bacteriol **189:**6293–6302. http://dx.doi.org/10.1128/JB.00546-07.
4. **Marquis RE.** 1995. Oxygen metabolism, oxidative stress and acid-base physiology of dental plaque biofilms. J Ind Microbiol **15:**198–207. http://dx.doi.org/10.1007/BF01569826.
5. **Bowden GH, Hamilton IR.** 1998. Survival of oral bacteria. Crit Rev Oral Biol Med **9:**54–85. http://dx.doi.org/10.1177/10454411980090010401.
6. **Ahn SJ, Rice KC, Oleas J, Bayles KW, Burne RA.** 2010. The *Streptococcus mutans* Cid and Lrg systems modulate virulence traits in response to multiple environmental signals. Microbiology **156:**3136–3147. http://dx.doi.org/10.1099/mic.0.039586-0.
7. **Jung CJ, Zheng QH, Shieh YH, Lin CS, Chia JS.** 2009. *Streptococcus mutans* auto AtlA is a fibronectin-binding protein and contributes to bacterial survival in the bloodstream and virulence for infective endocarditis. Mol Microbiol **74:**888–902. http://dx.doi.org/10.1111/j.1365-2958.2009.06903.x.
8. **Bayles KW.** 2007. The biological role of death and lysis in biofilm development. Nat Rev Microbiol **5:**721–726. http://dx.doi.org/10.1038/nrmicro1743.
9. **Bayles KW.** 2014. Bacterial programmed cell death: making sense of a paradox. Nat Rev Microbiol **12:**63–69. http://dx.doi.org/10.1038/nrmicro3136.
10. **Wang IN, Smith DL, Young R.** 2000. Holins: the protein clocks of bacteriophage infections. Annu Rev Microbiol **54:**799–825. http://dx.doi.org/10.1146/annurev.micro.54.1.799.
11. **Young R.** 2002. Bacteriophage holins: deadly diversity. J Mol Microbiol Biotechnol **4:**21–36.
12. **Young R, Blasi U.** 1995. Holins: form and function in bacteriophage lysis. FEMS Microbiol Rev **17:**191–205. http://dx.doi.org/10.1111/j.1574-6976.1995.tb00202.x.
13. **Groicher KH, Firek BA, Fujimoto DF, Bayles KW.** 2000. The *Staphylococcus aureus lrgAB* operon modulates murein hydrolase activity and penicillin tolerance. J Bacteriol **182:**1794–1801. http://dx.doi.org/10.1128/JB.182.7.1794-1801.2000.
14. **Rice KC, Bayles KW.** 2003. Death's toolbox: examining the molecular components of bacterial programmed cell death. Mol Microbiol **50:**729–738. http://dx.doi.org/10.1046/j.1365-2958.2003.t01-1-03720.x.
15. **Rice KC, Firek BA, Nelson JB, Yang SJ, Patton TG, Bayles KW.** 2003. The *Staphylococcus aureus cidAB* operon: evaluation of its role in regulation of murein hydrolase activity and penicillin tolerance. J Bacteriol **185:**2635–2643. http://dx.doi.org/10.1128/JB.185.8.2635-2643.2003.
16. **Ahn SJ, Qu MD, Roberts E, Burne RA, Rice KC.** 2012. Identification of the *Streptococcus mutans* LytST two-component regulon reveals its contribution to oxidative stress tolerance. BMC Microbiol **12:**187. http://dx.doi.org/10.1186/1471-2180-12-187.
17. **Ahn SJ, Wen ZT, Burne RA.** 2006. Multilevel control of competence development and stress tolerance in *Streptococcus mutans* UA159. Infect Immun **74:**1631–1642. http://dx.doi.org/10.1128/IAI.74.3.1631-1642.2006.
18. **Sambrook J, Fritsch EF, Maniatis T.** 1989. Molecular cloning: a laboratory manual, 2nd ed. Cold Spring Harbor Laboratory Press, Cold Spring Harbor, NY.
19. **Lau PC, Sung CK, Lee JH, Morrison DA, Cvitkovitch DG.** 2002. PCR ligation mutagenesis in transformable streptococci: application and efficiency. J Microbiol Methods **49:**193–205. http://dx.doi.org/10.1016/S0167-7012(01)00369-4.
20. **Biswas I, Jha JK, Fromm N.** 2008. Shuttle expression plasmids for genetic studies in *Streptococcus mutans*. Microbiology **154:**2275–2282. http://dx.doi.org/10.1099/mic.0.2008/019265-0.
21. **Zeng L, Burne RA.** 2015. Sucrose- and fructose-specific effects on the transcriptome of *Streptococcus mutans*, as determined by RNA sequencing. Appl Environ Microbiol **82:**146–156. http://dx.doi.org/10.1128/AEM.02681-15.
22. **Robinson MD, McCarthy DJ, Smyth GK.** 2010. edgeR: a Bioconductor package for differential expression analysis of digital gene expression data. Bioinformatics **26:**139–140. http://dx.doi.org/10.1093/bioinformatics/btp616.
23. **Gentleman RC, Carey VJ, Bates DM, Bolstad B, Dettling M, Dudoit S, Ellis B, Gautier L, Ge Y, Gentry J, Hornik K, Hothorn T, Huber W, Iacus S, Irizarry R, Leisch F, Li C, Maechler M, Rossini AJ, Sawitzki G, Smith C, Smyth G, Tierney L, Yang JY, Zhang J.** 2004. Bioconductor: open software development for computational biology and bioinformatics. Genome Biol **5:**R80. http://dx.doi.org/10.1186/gb-2004-5-10-r80.
24. **Huang DW, Sherman BT, Lempicki RA.** 2009. Systematic and integrative analysis of large gene lists using DAVID bioinformatics resources. Nat Protoc **4:**44–57. http://dx.doi.org/10.1038/nprot.2008.211.
25. **Huang DW, Sherman BT, Lempicki RA.** 2009. Bioinformatics enrichment tools: paths toward the comprehensive functional analysis of large gene lists. Nucleic Acids Res **37:**1–13. http://dx.doi.org/10.1093/nar/gkn923.
26. **Supek F, Bosnjak M, Skunca N, Smuc T.** 2011. REVIGO summarizes and visualizes long lists of gene ontology terms. PLoS One **6:**e21800. http://dx.doi.org/10.1371/journal.pone.0021800.
27. **Ahn SJ, Lemos JA, Burne RA.** 2005. Role of HtrA in growth and competence of *Streptococcus mutans* UA159. J Bacteriol **187:**3028–3038. http://dx.doi.org/10.1128/JB.187.9.3028-3038.2005.
28. **Ajdic D, McShan WM, McLaughlin RE, Savic G, Chang J, Carson MB, Primeaux C, Tian R, Kenton S, Jia H, Lin S, Qian Y, Li S, Zhu H, Najar F, Lai H, White J, Roe BA, Ferretti JJ.** 2002. Genome sequence of *Streptococcus mutans* UA159, a cariogenic dental pathogen. Proc Natl Acad Sci U S A **99:**14434–14439. http://dx.doi.org/10.1073/pnas.172501299.
29. **Wen ZT, Burne RA.** 2002. Analysis of *cis*- and *trans*-acting factors involved in regulation of the *Streptococcus mutans* fructanase gene (*fruA*). J Bacteriol **184:**126–133. http://dx.doi.org/10.1128/JB.184.1.126-133.2002.
30. **Dubrac S, Msadek T.** 2008. Tearing down the wall: peptidoglycan metabolism and the WalK/WalR (YycG/YycF) essential two-component system. Adv Exp Med Biol **631:**214–228. http://dx.doi.org/10.1007/978-0-387-78885-2_15.
31. **Echenique JR, Trombe MC.** 2001. Competence repression under oxygen limitation through the two-component MicAB signal-transducing system in *Streptococcus pneumoniae* and involvement of the PAS domain of MicB. J Bacteriol **183:**4599–4608. http://dx.doi.org/10.1128/JB.183.15.4599-4608.2001.
32. **Liu M, Hanks TS, Zhang J, McClure MJ, Siemsen DW, Elser JL, Quinn MT, Lei B.** 2006. Defects in ex vivo and in vivo growth and sensitivity to osmotic stress of group A *Streptococcus* caused by interruption of response regulator gene *vicR*. Microbiology **152:**967–978. http://dx.doi.org/10.1099/mic.0.28706-0.
33. **Martin PK, Li T, Sun D, Biek DP, Schmid MB.** 1999. Role in cell permeability of an essential two-component system in *Staphylococcus aureus*. J Bacteriol **181:**3666–3673.
34. **Senadheera MD, Guggenheim B, Spatafora GA, Huang YC, Choi J, Hung DC, Treglown JS, Goodman SD, Ellen RP, Cvitkovitch DG.** 2005. A VicRK signal transduction system in *Streptococcus mutans* affects *gtfBCD*, *gbpB*, and *ftf* expression, biofilm formation, and genetic competence development. J Bacteriol **187:**4064–4076. http://dx.doi.org/10.1128/JB.187.12.4064-4076.2005.
35. **Throup JP, Koretke KK, Bryant AP, Ingraham KA, Chalker AF, Ge Y, Marra A, Wallis NG, Brown JR, Holmes DJ, Rosenberg M, Burnham MK.** 2000. A genomic analysis of two-component signal transduction in *Streptococcus pneumoniae*. Mol Microbiol **35:**566–576.
36. **Wagner C, de Saizieu A, Schonfeld HJ, Kamber M, Lange R, Thompson CJ, Page MG.** 2002. Genetic analysis and functional characterization of

the *Streptococcus pneumoniae vic* operon. Infect Immun **70:**6121–6128. http://dx.doi.org/10.1128/IAI.70.11.6121-6128.2002.
37. **Dubrac S, Bisicchia P, Devine KM, Msadek T.** 2008. A matter of life and death: cell wall homeostasis and the WalKR (YycGF) essential signal transduction pathway. Mol Microbiol **70:**1307–1322. http://dx.doi.org/10.1111/j.1365-2958.2008.06483.x.
38. **Senadheera DB, Cordova M, Ayala EA, Chavez de Paz LE, Singh K, Downey JS, Svensater G, Goodman SD, Cvitkovitch DG.** 2012. Regulation of bacteriocin production and cell death by the VicRK signaling system in *Streptococcus mutans*. J Bacteriol **194:**1307–1316. http://dx.doi.org/10.1128/JB.06071-11.
39. **Deng DM, Liu MJ, ten Cate JM, Crielaard W.** 2007. The VicRK system of *Streptococcus mutans* responds to oxidative stress. J Dent Res **86:**606–610. http://dx.doi.org/10.1177/154405910708600705.
40. **Friedman L, Alder JD, Silverman JA.** 2006. Genetic changes that correlate with reduced susceptibility to daptomycin in *Staphylococcus aureus*. Antimicrob Agents Chemother **50:**2137–2145. http://dx.doi.org/10.1128/AAC.00039-06.
41. **Jansen A, Turck M, Szekat C, Nagel M, Clever I, Bierbaum G.** 2007. Role of insertion elements and *yycFG* in the development of decreased susceptibility to vancomycin in *Staphylococcus aureus*. Int J Med Microbiol **297:**205–215. http://dx.doi.org/10.1016/j.ijmm.2007.02.002.
42. **Kadioglu A, Echenique J, Manco S, Trombe MC, Andrew PW.** 2003. The MicAB two-component signaling system is involved in virulence of *Streptococcus pneumoniae*. Infect Immun **71:**6676–6679. http://dx.doi.org/10.1128/IAI.71.11.6676-6679.2003.
43. **Dubrac S, Boneca IG, Poupel O, Msadek T.** 2007. New insights into the WalK/WalR (YycG/YycF) essential signal transduction pathway reveal a major role in controlling cell wall metabolism and biofilm formation in *Staphylococcus aureus*. J Bacteriol **189:**8257–8269. http://dx.doi.org/10.1128/JB.00645-07.
44. **Taylor BL, Zhulin IB.** 1999. PAS domains: internal sensors of oxygen, redox potential, and light. Microbiol Mol Biol Rev **63:**479–506.
45. **Novick RP, Ram G.** 2016. The floating (pathogenicity) island: a genomic dessert. Trends Genet **32:**114–126. http://dx.doi.org/10.1016/j.tig.2015.11.005.
46. **Langille MG, Hsiao WW, Brinkman FS.** 2010. Detecting genomic islands using bioinformatics approaches. Nat Rev Microbiol **8:**373–382. http://dx.doi.org/10.1038/nrmicro2350.
47. **Wu C, Cichewicz R, Li Y, Liu J, Roe B, Ferretti J, Merritt J, Qi F.** 2010. Genomic island TnSmu2 of *Streptococcus mutans* harbors a nonribosomal peptide synthetase-polyketide synthase gene cluster responsible for the biosynthesis of pigments involved in oxygen and H_2O_2 tolerance. Appl Environ Microbiol **76:**5815–5826. http://dx.doi.org/10.1128/AEM.03079-09.
48. **Barrangou R, Fremaux C, Deveau H, Richards M, Boyaval P, Moineau S, Romero DA, Horvath P.** 2007. CRISPR provides acquired resistance against viruses in prokaryotes. Science **315:**1709–1712. http://dx.doi.org/10.1126/science.1138140.
49. **Deveau H, Garneau JE, Moineau S.** 2010. CRISPR/Cas system and its role in phage-bacteria interactions. Annu Rev Microbiol **64:**475–493. http://dx.doi.org/10.1146/annurev.micro.112408.134123.
50. **Horvath P, Barrangou R.** 2010. CRISPR/Cas, the immune system of bacteria and archaea. Science **327:**167–170. http://dx.doi.org/10.1126/science.1179555.
51. **Louwen R, Staals RH, Endtz HP, van Baarlen P, van der Oost J.** 2014. The role of CRISPR-Cas systems in virulence of pathogenic bacteria. Microbiol Mol Biol Rev **78:**74–88. http://dx.doi.org/10.1128/MMBR.00039-13.
52. **Marraffini LA.** 2015. CRISPR-Cas immunity in prokaryotes. Nature **526:**55–61. http://dx.doi.org/10.1038/nature15386.
53. **Serbanescu MA, Cordova M, Krastel K, Flick R, Beloglazova N, Latos A, Yakunin AF, Senadheera DB, Cvitkovitch DG.** 2015. Role of the *Streptococcus mutans* CRISPR-Cas systems in immunity and cell physiology. J Bacteriol **197:**749–761. http://dx.doi.org/10.1128/JB.02333-14.
54. **van der Ploeg JR.** 2009. Analysis of CRISPR in *Streptococcus mutans* suggests frequent occurrence of acquired immunity against infection by M102-like bacteriophages. Microbiology **155:**1966–1976. http://dx.doi.org/10.1099/mic.0.027508-0.
55. **Lewis K.** 2008. Multidrug tolerance of biofilms and persister cells. Curr Top Microbiol Immunol **322:**107–131.
56. **Lewis K.** 2010. Persister cells. Annu Rev Microbiol **64:**357–372. http://dx.doi.org/10.1146/annurev.micro.112408.134306.
57. **Prax M, Bertram R.** 2014. Metabolic aspects of bacterial persisters. Front Cell Infect Microbiol **4:**148. http://dx.doi.org/10.1038/nprot.2008.211.
58. **Wu Y, Vulic M, Keren I, Lewis K.** 2012. Role of oxidative stress in persister tolerance. Antimicrob Agents Chemother **56:**4922–4926. http://dx.doi.org/10.1128/AAC.00921-12.
59. **Syed MA, Koyanagi S, Sharma E, Jobin MC, Yakunin AF, Levesque CM.** 2011. The chromosomal *mazEF* locus of *Streptococcus mutans* encodes a functional type II toxin-antitoxin addiction system. J Bacteriol **193:**1122–1130. http://dx.doi.org/10.1128/JB.01114-10.
60. **Sevin EW, Barloy-Hubler F.** 2007. RASTA-Bacteria: a web-based tool for identifying toxin-antitoxin loci in prokaryotes. Genome Biol **8:**R155. http://dx.doi.org/10.1186/gb-2007-8-8-r155.
61. **Page R, Peti W.** 2016. Toxin-antitoxin systems in bacterial growth arrest and persistence. Nat Chem Biol **12:**208–214. http://dx.doi.org/10.1038/nchembio.2044.
62. **Schuster CF, Bertram R.** 2013. Toxin-antitoxin systems are ubiquitous and versatile modulators of prokaryotic cell fate. FEMS Microbiol Lett **340:**73–85. http://dx.doi.org/10.1111/1574-6968.12074.
63. **Wang X, Wood TK.** 2011. Toxin-antitoxin systems influence biofilm and persister cell formation and the general stress response. Appl Environ Microbiol **77:**5577–5583. http://dx.doi.org/10.1128/AEM.05068-11.
64. **Wood TK.** 2016. Combatting bacterial persister cells. Biotechnol Bioeng **113:**476–483. http://dx.doi.org/10.1002/bit.25721.
65. **Maisonneuve E, Castro-Camargo M, Gerdes K.** 2013. (p)ppGpp controls bacterial persistence by stochastic induction of toxin-antitoxin activity. Cell **154:**1140–1150. http://dx.doi.org/10.1016/j.cell.2013.07.048.
66. **Martinez LC, Vadyvaloo V.** 2014. Mechanisms of post-transcriptional gene regulation in bacterial biofilms. Front Cell Infect Microbiol **4:**38. http://dx.doi.org/10.3389/fcimb.2014.00038.